

In presenting the dissertation as a partial fulfillment of the requirements for an advanced degree from the Georgia Institute of Technology, I agree that the Library of the Institute shall make it available for inspection and circulation in accordance with its regulations governing materials of this type. I agree that permission to copy from, or to publish from, this dissertation may be granted by the professor under whose direction it was written, or, in his absence, by the Dean of the Graduate Division when such copying or publication is solely for scholarly purposes and does not involve potential financial gain. It is understood that any copying from, or publication of, this dissertation which involves potential financial gain will not be allowed without written permission.

3/17/65

b

LABORATORY INVESTIGATION OF THE BEARING
CAPACITY OF A TWO LAYER SYSTEM BY USING
CIRCULAR AND SQUARE MODEL FOOTINGS

A THESIS

Presented to

The Faculty of the Graduate Division

by

Polidoro Velasco C

In Partial Fulfillment


of the Requirements for the Degree


Master of Science in Civil Engineering

Georgia Institute of Technology

June, 1967

LABORATORY INVESTIGATION OF THE BEARING
CAPACITY OF A TWO LAYER SYSTEM BY USING
CIRCULAR AND SQUARE MODEL FOOTINGS

Approved: 

Chairman 

Date approved by Chairman: 5/31/67

TABLE OF CONTENTS

	Page
ACKNOWLEDGMENTS	ii
LIST OF ILLUSTRATIONS	iii
LIST OF TABLES	iv
SUMMARY	v
Chapter	
I. INTRODUCTION	1
Purpose of Research	
II. THEORETICAL CONSIDERATIONS	3
Ultimate Bearing Capacity	
Homogeneous Soil	
Two Layer System	
III. EQUIPMENT AND PROCEDURE	11
Hard Layer	
Unconfined Compressive Strength, Apparent	
Cohesion, and Apparent Angle of Internal	
Friction	
Secant Modulus of Elasticity	
Modulus of Rupture	
Soft Layer	
Procedure	
IV. DISCUSSION	17
Ultimate Bearing Capacity	
Mechanism of Failure	
Punching Failure	
Flexural Failure	
Theoretical and Test Results Comparison	
V. CONCLUSIONS	35
VI. RECOMMENDATIONS	37

REFERENCES.....	Page 38
APPENDIX I	40
APPENDIX II	54

ACKNOWLEDGMENTS

The writer wishes to express his appreciation to Professor George F. Sowers for his encouragement during the course of this research.

To Dr. Neil H. Wade and Dr. Billy B. Mazanti, many thanks are extended for their guidance and helpful comments throughout the research.

LIST OF ILLUSTRATIONS

Figure	Page
1. Logarithmic Spiral Analysis	6
2. Effect of Footing Size on the Ultimate Bearing Capacity of the System - Square Footings	18
3. Effect of Footing Size on the Ultimate Bearing Capacity of the System - Circular Footings	19
4. Effect of Hard Layer Thickness on the Ultimate Bearing Capacity of the System	21
5. Graph Showing Influence of Footing Area on the Ultimate Bearing Capacity	22
6. Flexural Failure	23
7. Hard Layer after Failure - Punching Failure	24
8. Hard Layer after Failure - Punching Failure	25
9. Hard Layer after Failure - Flexural Failure	27
10. Hard Layer after Failure - Flexural Failure	28
11. Punching Failure	29
12. Results of Loading Tests and Theoretical Values ..	31
13. Modulus of Elasticity of the Plaster-Sand Mixture	34
Appendix I - Cracks on Top of Hard Layer after Failure According to Size of Footing and Thickness Of the Hard Layer	40
Appendix II - Bearing Pressure Settlement Curves	54

LIST OF TABLES

Table	Page
I. Properties of the Plaster-Sand Mixture.....	12
II. Properties of the Clay.....	15
III. Coefficient of Subgrade Reaction.....	33

SUMMARY

The purpose of the investigation was to determine experimentally the relationship between ultimate bearing capacity and the size and shape of footings bearing on a hard layer overlying a soft layer.

The hard layer consisted of a mixture of gypsum plaster, sand and water. The soft layer consisted of equal parts of bentonite, kaolinite, and water.

Static load tests were conducted to determine the ultimate bearing capacity of the two-layer system, using square and circular model footings having one, two and three inches as width and diameter respectively. The footings were one inch thick and made from steel.

To study the influence of the thickness of the hard layer on the bearing capacity, the tests were conducted over one half inch, three quarter inch, and one inch thick slabs placed on the surface of the clay. The slabs were 22 inches long by 22 inches wide.

Ultimate bearing capacity was taken as the average bearing pressure at which failure, or sudden sinking of the footing, took place.

It was found that the ultimate bearing capacity of a layered system is related to the ratio, $\frac{B}{H}$, in which B is the width or diameter of the footings and H is the thickness of

the hard layer. As the value of $\frac{B}{H}$ increased (increase in B for a constant H) the ultimate bearing capacity of the system decreased.

The nature of failure was not the same for all the tests but was related to the size and shape of the footings and to the thickness of the hard layer. Accordingly, two types of failures were found to occur, a punching failure and a flexural failure.

The punching failure occurred when the thinner slab, 1/2 inch thick, was loaded with the one-inch diameter and the one-inch square footings.

With circular footings, which diameters were greater than one inch, the one half-inch thick slab cracked first along the two main directions and then suddenly broke approximately circular at a distance from the perimeter of the footing of about the footing diameter. When the thickness of the slab was increased to one inch the slab failed in flexure along two cracks that followed the directions of the two main dimensions of the slab.

With square footings failure began by yielding or cracking of the slab starting progressively from one of the corners of the footings and extending to the other corners.

The bearing capacity of the system increased as the thickness of the hard layer increases. The increase in bearing capacity due to the increase in thickness of the hard layer was more pronounced with the smaller footings than with the

larger footings. The increase in bearing capacity with increasing thickness was non-linear and followed a highly concave downward curve with circular and square footings having one inch as diameter and width respectively.

With increasing footing sizes, the increase in bearing capacity for the thicker layers was small and followed a slightly concave upward curve.

The ultimate bearing capacity of the hard layer alone was 72 per cent greater than the ultimate bearing capacity of the soft layer.

CHAPTER I

INTRODUCTION

The design of foundations must satisfy two main requirements; namely, the soil beneath the foundation must not fail and the total settlement of the foundation must be kept within limits that can be tolerated by the superstructure. This study is concerned only with the failure of the foundation.

When footings are founded on the surface of a hard stratum which overlies a soft stratum, the pressure applied at the footing level spreads out with increasing depth, and thus the induced pressures reaching the soft stratum will depend on the thickness of the hard stratum as well as on its ability to spread the load.

Besides the structural features of the hard layer, it is evident that the most relevant information in any investigation of this type is the relationship between bearing capacity and the thickness of the layer and the size and shape of the footings through which the loads are transferred to the ground.

Purpose of Research

Because of the large number of factors which affect the

bearing capacity of any two layer system, it is evident that any investigations which are to provide results of practical significance must be carried out in situ. It is equally evident, however, that these factors must be evaluated if any understanding of the basic relationship is to be achieved; and, this evaluation cannot easily be obtained in the field. Laboratory investigations are the obvious answer to the difficulty of providing the essential link between theoretical hypothesis and actual behavior. This work attempts to further the little which has been done in this field. The goal is to determine experimentally the relationship between bearing capacity and thickness of the hard stratum and bearing capacity and size and shape of footings through which the loads are transmitted to the foundation.

The materials used in these tests were a mixture of gypsum-plaster and sand, which was brittle and strong, and a mixture of bentonite and kaolinite that was very soft, with a low modulus of elasticity, E , and large strain at failure.

CHAPTER II

THEORETICAL CONSIDERATIONS

Ultimate Bearing Capacity

The ultimate bearing capacity of a material is defined as the average contact pressure between the footing and the material at which shear failure takes place. Most theories for ultimate bearing capacity are based on the behavior of an ideal homogeneous isotropic plastic material.

Homogeneous Soil

For a footing resting on the surface of such an ideal homogeneous and isotropic material, the generally accepted formulas for ultimate bearing capacity are: (Ref. 5)

Strip Footing:

$$q_u = cN_c + 0.5 B\gamma N_r \quad (1)$$

Square Footing:

$$q_u = 1.3 cN_c + 0.4 B\gamma N_r \quad (2)$$

Circular Footing:

$$q_u = 1.3 cN_c + 0.3 B\gamma N_r \quad (3)$$

where:

- q_u = ultimate bearing capacity
 c = cohesion of the material
 γ = unit weight of the material
 B = linear dimension of footing, width or diameter
 ϕ = angle of internal friction of the material
 N_c, N_r = factors depending upon the angle of internal friction of the material.

Two Layer System

The cylindrical failure surface proposed by Fellenius for the determination of the stability of a homogeneous soil has been used by S. J. Button (Ref. 10) to find the bearing capacity of infinitely long footings on a two-layer cohesive subsoil ($\phi = 0$). The ultimate bearing capacity is obtained by equating the moment of applied load about the center of the critical circular - arc to the reaction moment about the same point. The reaction moment is given by the summation of the total tangential shearing resistance, s , given by the well known Coulomb equation

$$s = c + n \tan \phi \quad (4)$$

multiplied by the radius of the arc. The magnitude of the normal pressure component " $n \tan \phi$ " acting on each element of the circular arc is not definitely known. To avoid this difficulty Button limited the Fellenius' method to homogeneous cohesive soils for which the angle of internal friction $\phi = 0$, so

" $n \tan \phi = 0$ ".

Unfortunately, the Button method applies only to long strip footing; whereas, in our investigation we are dealing with square and circular footings. This method does not consider relative strain, and the effect of non-simultaneous mobilization of shear in the two materials.

McLeod Method

The method of McLeod (Ref. 2) includes c and ϕ of the two materials and is similarly applied only to strip footings. McLeod used in his method the logarithmic-spiral failure surface. Calculation of the bearing capacity using the log-spiral involves balancing moments about the origin of the spiral. The resultants of the normal forces " n " and the friction forces " $n \tan \phi$ " pass through the origin. Thus, the forces tending to cause movement are the applied pressure " p " plus the weight of foundation material to the left of the origin within the spiral. The resisting forces are cohesion, acting along the surface of sliding, and the weight of material to the right of the origin within the spiral. (Figure 1)

In essence, McLeod's method involves the determination of c and ϕ values for an equivalent homogeneous material having the same ultimate strength as the layered system. The ultimate bearing capacity of this equivalent homogeneous material can then be calculated on the basis of a logarithmic spiral failure surface. The entire procedure requires a trial-and-error approach involving the use of successive approximations.

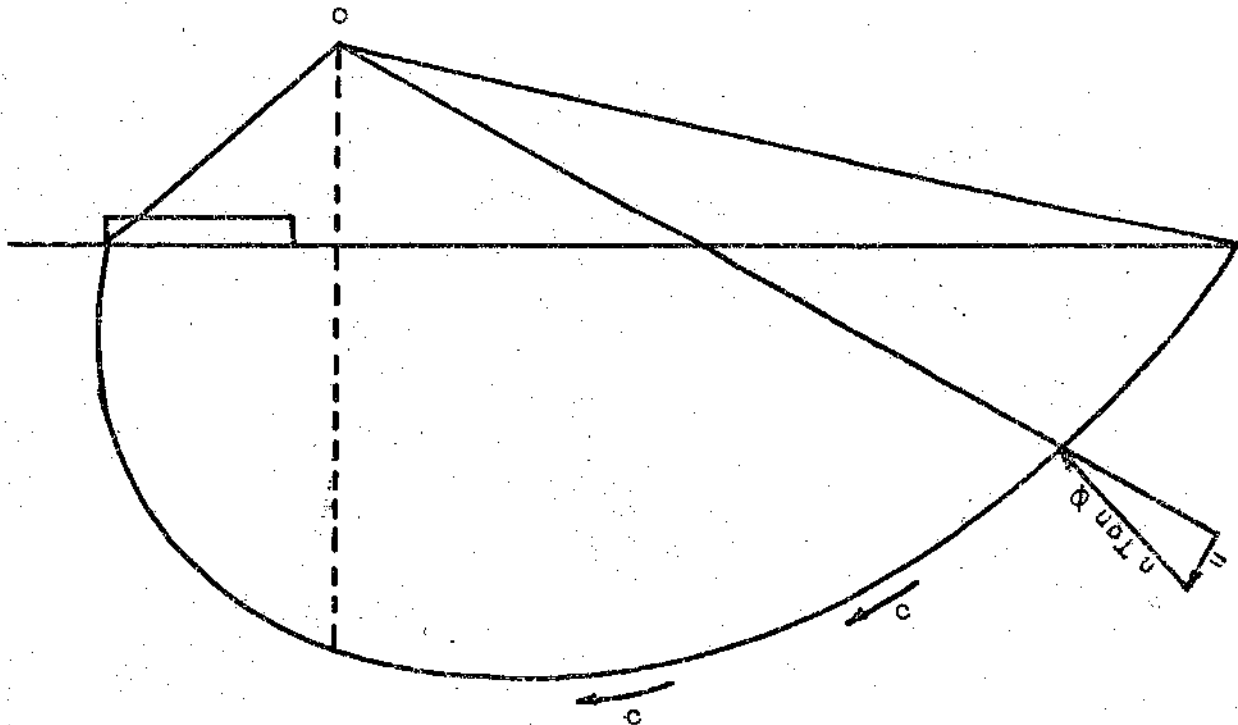


Figure 1: Logarithmic Spiral Analysis

Because this method is applicable only to strip footings, a detailed study of it will not be useful in our case, where circular and square footings are used.

Burmister Theory

Burmister (Ref. 1) provided a method of determining elastic stresses and displacement in a semi-infinite mass where that mass contained two materials of different modulus of elasticity. His solution to the two layered system is based on the application of the theory of elasticity so that the following assumptions and conditions are necessary:

- (1) The material in each layer is assumed to be homogeneous and isotropic and to follow Hooke's law.
- (2) The top layer of the two-layered system is assumed to be weightless and infinite in a horizontal direction but of finite thickness. The second layer is assumed infinite horizontally and in a vertically downward direction.
- (3) The boundary conditions assume the surface to be free of normal and shearing stresses outside the loaded area and that the displacement and stresses are zero at an infinite depth.
- (4) To satisfy continuity conditions it is assumed that the two layers are continuously in contact and act together as an elastic medium of composite nature.

- (5) The second layer is assumed to provide continuous uniform support for the top layer.
- (6) Failure conditions do not exist.

In relation to this investigation the principal criticism of the Burmister theory concerns its assumption that the two materials that make up the two-layered system function as perfectly elastic materials. This, as it is known, is not the case when dealing with a bearing capacity problem which deals with the ultimate strength of the materials, which is well beyond any elastic range of loading.

Meyerhof Analysis

G. G. Meyerhof (Ref. 7, 8) has presented a mathematical approach to the determination of ultimate failure loads for rigid slabs on an elastic subgrade. An estimate of the ultimate load is obtained from an ultimate strength analysis of slabs on the basis of plastic theory. The author uses his method to estimate the ultimate bearing capacity of rigid pavements under concentrated central, edge, and corner loads acting on the pavement. In the present investigation a comparison will be made between the values obtained from Meyerhof's method and the experimental results for a central load acting on a circular area.

Central Load - Circular Bearing Area

When a central concentrated load, much less than the ultimate is applied over a small circular area on a large rigid

slab in full contact with the base, the stresses and deflections of the slab can be computed as for an elastic and infinite plate on an elastic subgrade. As the load increases, the bending stresses below the load become equal to the flexural strength of the rigid material and the slab begins to yield which leads to radial tension cracks at the bottom. The maximum yield moment of resistance of the slab per unit length is given by Meyerhof as

$$M_y = \frac{f_b h^2}{6} \quad (5)$$

in which f_b is the flexural strength of the rigid material and h is the slab thickness.

The collapse or failure load is given by Meyerhof as

$$P_o = 2 M_o \pi \text{ for } R = 0 \quad (6)$$

and

$$P_o = \frac{4 M_o \pi}{1 - \frac{R}{3L}} \text{ for } \frac{R}{L} > 0.2 \quad (7)$$

where

P_o = collapse load

$M_o = M_y$ limit moment of resistance of slab per unit length

R = contact radius of load

$L = \left(\frac{E h^3}{12(1 - \nu^2) K} \right)^{\frac{1}{4}}$ radius of relative stiffness of slab

E = Modulus of elasticity of slab

K = Modulus of subgrade reaction

ν = Poisson's ratio of slab

CHAPTER III

EQUIPMENT AND PROCEDURE

The model footings used in the tests consisted of circular and square models of steel, of one inch, two inch, and three inch diameter and width, respectively. The thickness of the model footings was one inch. The materials used to make up the two layer system were gypsum plaster, sand and a mixture of equal parts by weight of dry bentonite and kaolinite clays, and water.

Hard Layer

The hard layer was a mixture of plaster sand and water. To minimize scatter in the results the sand was carefully selected and graded. It was dried and sieved, and that passing the No. 14 sieve was used in the mixture of plaster, sand and water. The mixture was weight controlled in the proportion of 1:3:1, plaster: sand: water. This is more accurate than a volume proportion since volume would change according to the density of packing. The sand plaster product was a relatively hard brittle material with the following average properties:

Table 1. Properties of the Plaster-Sand Mixture

Unconfined compressive strength:	216 psi
Apparent cohesion:	102 psi
Apparent angle of internal friction:	4
Secant Modulus of elasticity:	13,000 psi
Modulus of rupture:	120 psi

Unconfined Compressive Strength, Apparent Cohesion, and
Apparent Angle of Internal Friction

These values were found using cylindrical specimens, 1 3/8 inch diameter and 3 3/4 inch high. The specimens were allowed to set for one day, the same time as for the slabs tested. Unconfined and confined tests using 20 psi and 40 psi were run in a triaxial cell.

Secant Modulus of Elasticity

There is no standard method of determining the secant modulus; for instance, in some laboratories the secant modulus of elasticity of concrete is measured at stresses representing 15, 25, 33 or 50 per cent of the ultimate strength (Ref. 12).

Because the secant modulus decreases with an increase in stress, the stress at which the modulus has been determined should always be stated. In this investigation the secant modulus represents the average value of tests measured at 25 per cent of the ultimate strength, Figure 13.

Modulus of Rupture

The value of flexural strength is necessary in estimating the ultimate load as given in Meyerhof analysis. The flexural strength can be measured by subjecting a beam to flexure. The theoretical maximum tensile stress reached in the bottom fibre of the test beam is known as the modulus of rupture. Here "theoretical" refers to the assumption in the calculation of the modulus of rupture that stress is proportional to the distance from the neutral axis of the beam while the shape of the actual stress block under loads nearing failure is known not to be triangular. According to experiments made with concrete (Ref. 13), the modulus of rupture thus obtained overestimates the tensile strength of concrete and gives a higher value than would be obtained in a direct tension test on a cylinder made of the same concrete.

In this investigation a symmetrical two-point loading, which produces a constant bending moment between the load points, was used. With this arrangement of loading, a fact of the bottom surface of the beam, one-third of the span, is subjected to the maximum stress, and failure may start at any section not strong enough to resist this stress. On the other hand, if a central point load were used failure would generally occur only when the strength of the fibre immediately under the load is exceeded. It can be seen that the probability of a weak element being subjected to the critical stress is

considerably greater under two point loading than when a central load acts.

Several third-point loadings on 1 by 1 by 11 1/4 inch beams supported over a span of 10 inches were run. The modulus of rupture was calculated on the basis of elastic theory:

$$f_b = \frac{PL}{bd^2} \quad (8)$$

where

P = Maximum total load on the beam

L = Span

b = width of the beam

d = depth of the beam

Since $b = d = 1"$ and $L = 10"$ $f_b = 10P$.

A wood and plexiglass form was used to cast the slabs. The slabs were 22" by 22" in plan and varied in thickness, 1/2", 3/4" and 1" thick. They were allowed to harden for one day and then were tested.

Soft Layer

The soft layer consisted of equal parts of bentonite and kaolinite clays, and water.

The average physical properties were:

Table III. Properties of the Clay

Water Content:	82.5%
Unconfined Strength: q_u	405 psf
Secant Modulus at $\frac{q_u}{2}$:	65.5 psi
Strain at failure:	7.4%

Procedure

A sturdy steel box 24 inches by 24 inches in cross-section and 20 inches deep was used for housing the clay mass and hard layer. A steel beam was located over the top of the steel box. Attached to the steel beam and situated over the center point of the box was a ball-bearing housing providing a practically frictionless enclosure for a stainless steel rod. Attached to the loading rod was a platform used for holding the weights for loading. Weights of 5, 10 and 20 lbs. were used. Attached to the loading rod was a micrometer dial gage for measuring settlements at the center of each footing. The clay mixture was placed in the steel box in 4 inch thick lifts until the depth of the clay was 18 inches. After the clay stratum had been prepared, the surface was carefully leveled with an aluminum straightedge to insure contact between the two layers at all points to avoid discontinuities which have great influence in the distribution of stresses. The plaster-sand slab was placed on the surface of the clay and the model

footing was set at the center of the slab. Next, loads were applied to the system by means of the weight blocks. The footing was allowed to settle under each load increment until settlement practically stopped. As the failure load condition was approached as indicated by greater settlement per load, the incremental load value was reduced and loading continued until failure occurred.

After the failure, all the cracks on the top of the slab were carefully measured so that a sketch could be made. Next, the load was removed and the crack pattern on bottom of the slab was studied. The clay was removed to a depth of 12 inches and replaced in 4 inch thick lifts. After the clay stratum was prepared, the following test was run as before, and the same procedure was repeated for each test run.

CHAPTER IV

DISCUSSION

The purpose of this investigation was to study experimentally the relationship between the ultimate bearing capacity of a hard layer overlying a soft layer, and the size and shape of footings through which the load was transmitted to the system, as well as the influence of the thickness of the hard layer over the ultimate bearing capacity.

Ultimate Bearing Capacity

The ultimate bearing capacity of the system was taken as the load which produced a total collapse of the hard layer, divided by the area of the footing used.

To compare the ultimate bearing capacity of the system as a whole with the bearing capacity of each individual layer formulas (2) and (3) were used, based on the results of tri-axial and unconfined shear test performed in each material.

Clay

The ultimate bearing capacity for circular and square footings on clay is given by:

$$q_u = 1.3 c N_c$$

$$c = \text{cohesion of the clay}$$

$$N_c = \text{factor depending on the angle of internal}$$

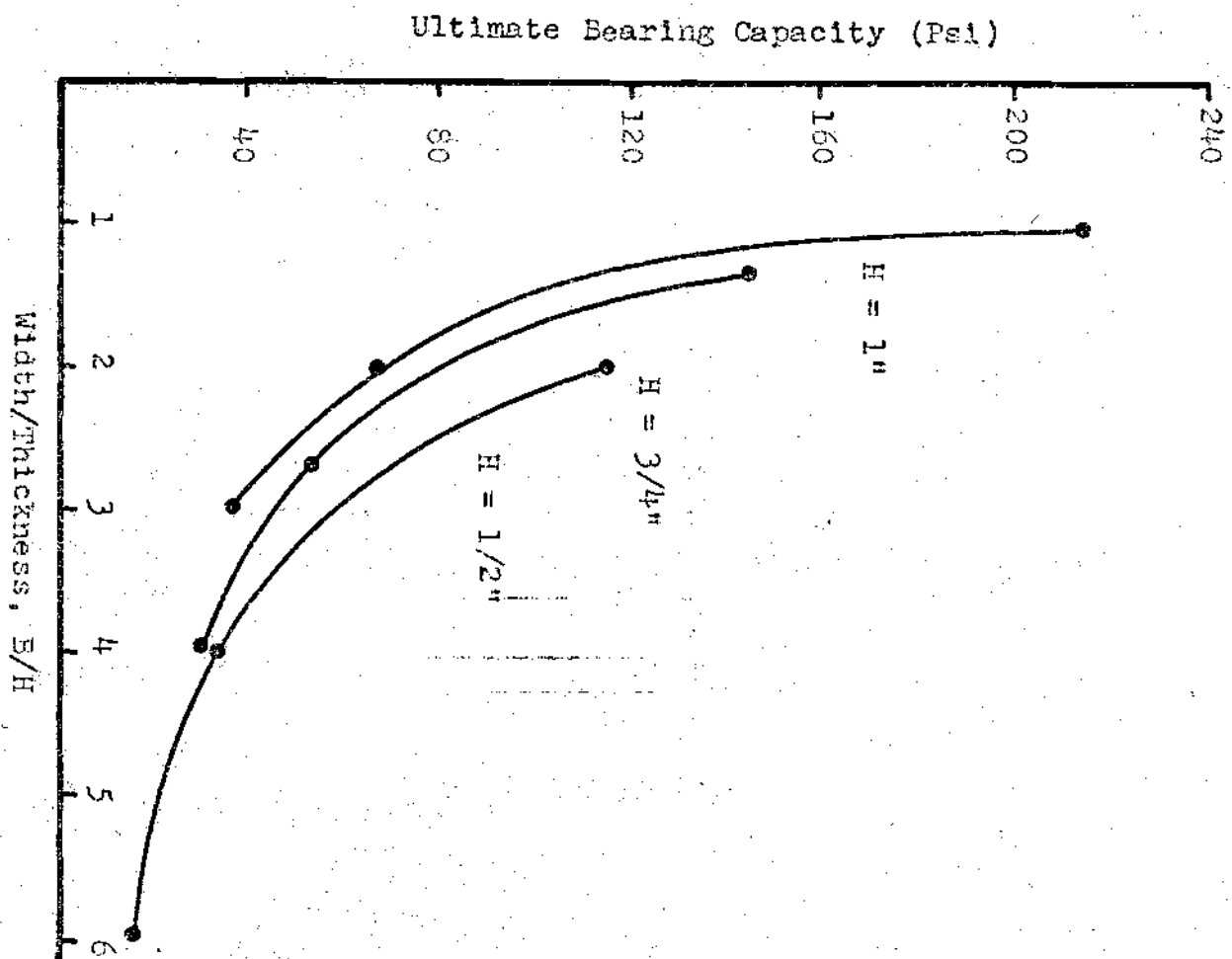


Figure 2: Effect of Footing Size on the Ultimate Bearing Capacity of the System - Square Footings

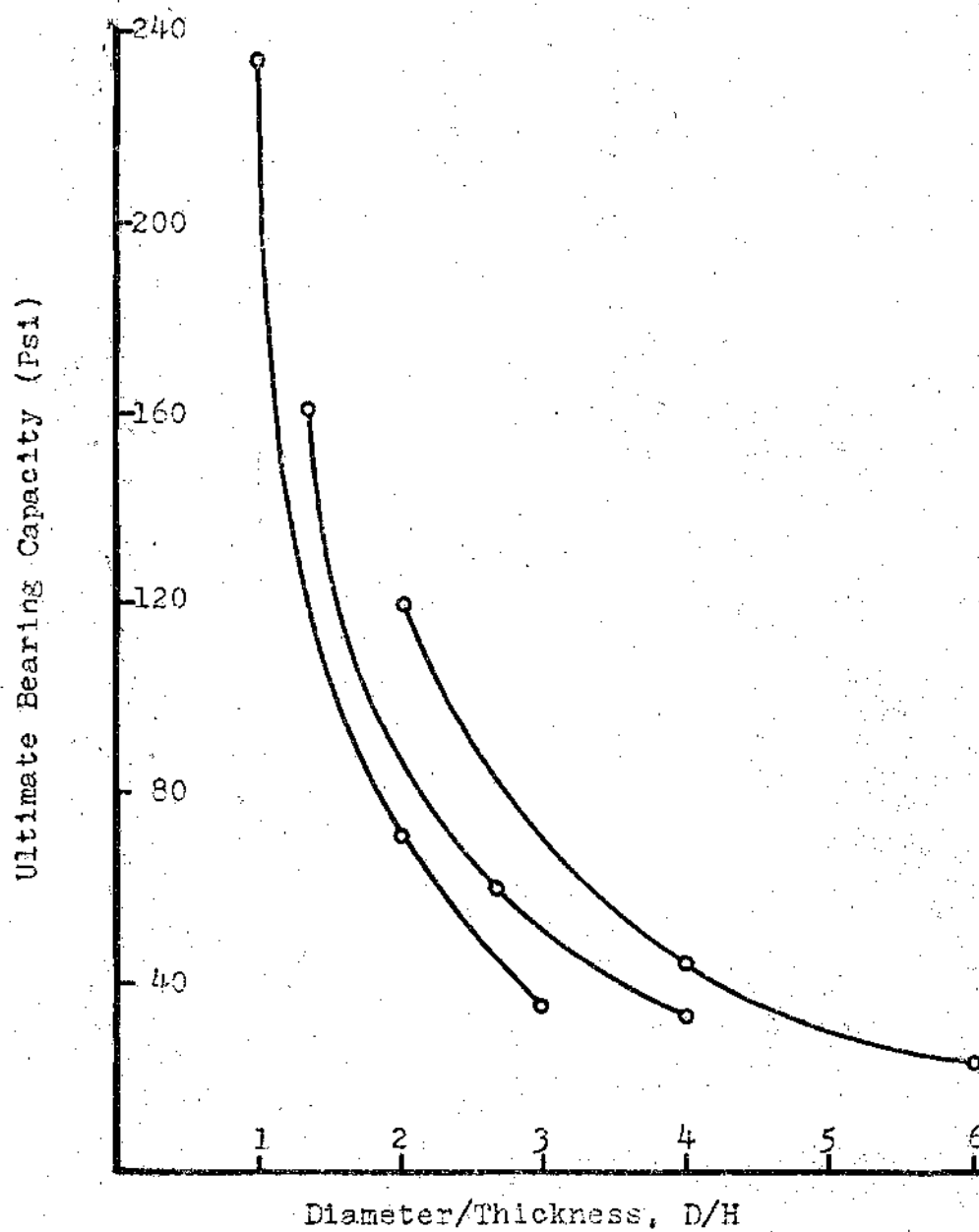


Figure 3: Effect of Footing Size on the Ultimate Bearing Capacity of the System - Circular Footings.

friction of the clay

$$\text{For } \phi = 0 \quad N_c = 5.7$$

$$c = 1.41 \text{ psi}$$

$$q_u = 1.3 \times 1.4 \times 5.7 = 10.5 \text{ psi}$$

Plaster-sand Mixture

Using formulas (2) and (3) for $\phi = 4$ we have
and $N_c = 5.7$.

$$q_u = 1.3 \times c \times N_c = 1.3 \times 102 \times 5.7 = 755 \text{ psi}$$

Two tests were run on a block 8 inches by 8 inches in cross-section and 12 inches deep. Using a circular footing having 1 inch as diameter the ultimate bearing capacity was 780 psi and with a square footing 1 inch wide the average ultimate bearing capacity was 745 psi, which is in close agreement with the theoretical value obtained.

Shape of Footing

According to Figure 4, it appears as if circular footings give slightly higher values of ultimate bearing capacity. However, this may not be true since this difference may be attributed to the difference in magnitude of contact area. According to Figure 5, the ultimate bearing capacity of the system increases as the ratio of area over thickness of hard layer decreases. Here it can be seen that as the area increases the ultimate bearing capacity decreases in a non-linear pattern. This decrease appears to be independent of the shape of the footing and of the thickness of the hard layer since all the points appear to have a common focus.

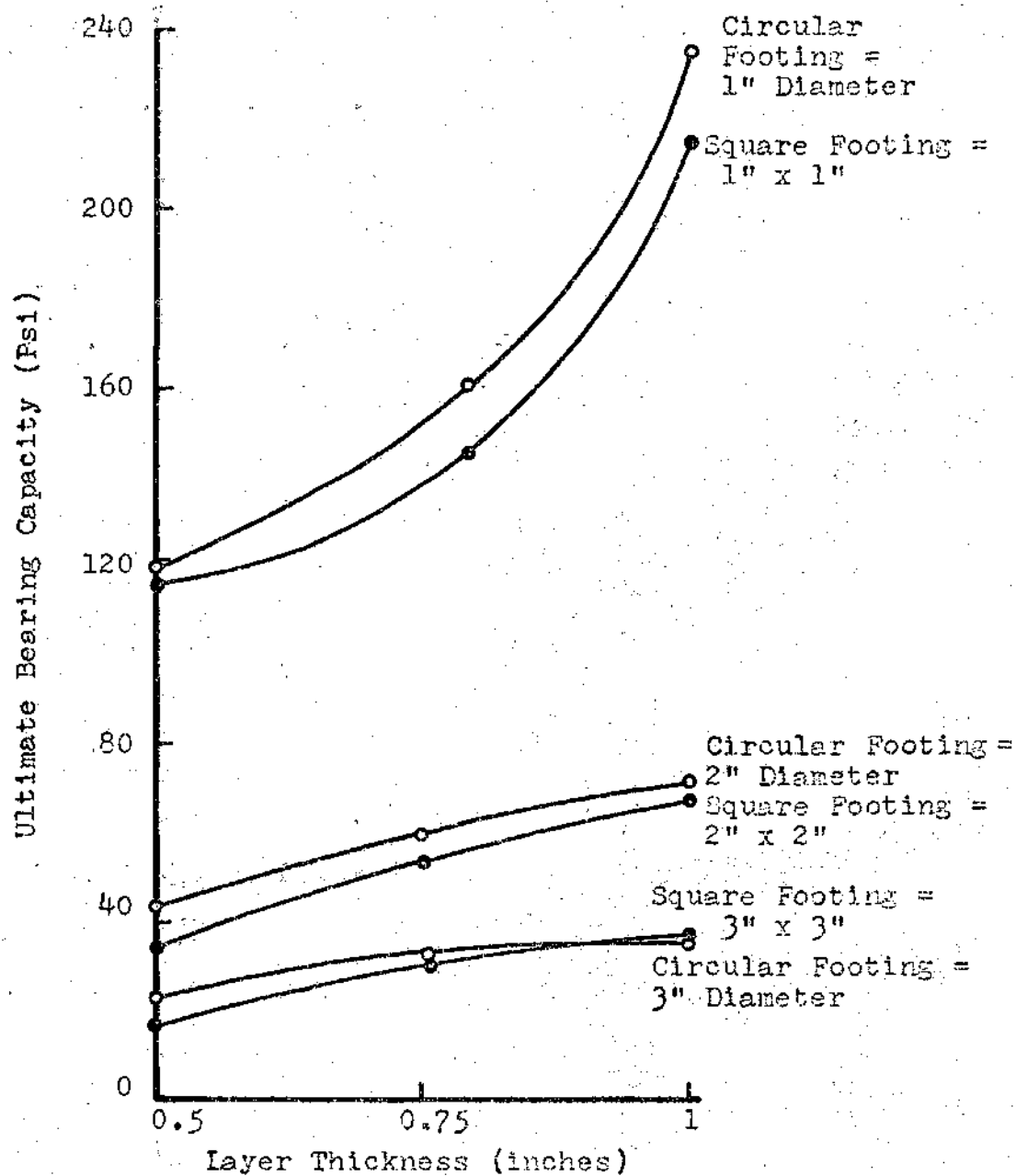


Figure 4: Effect of Hard Layer Thickness on the Ultimate Bearing Capacity of the System

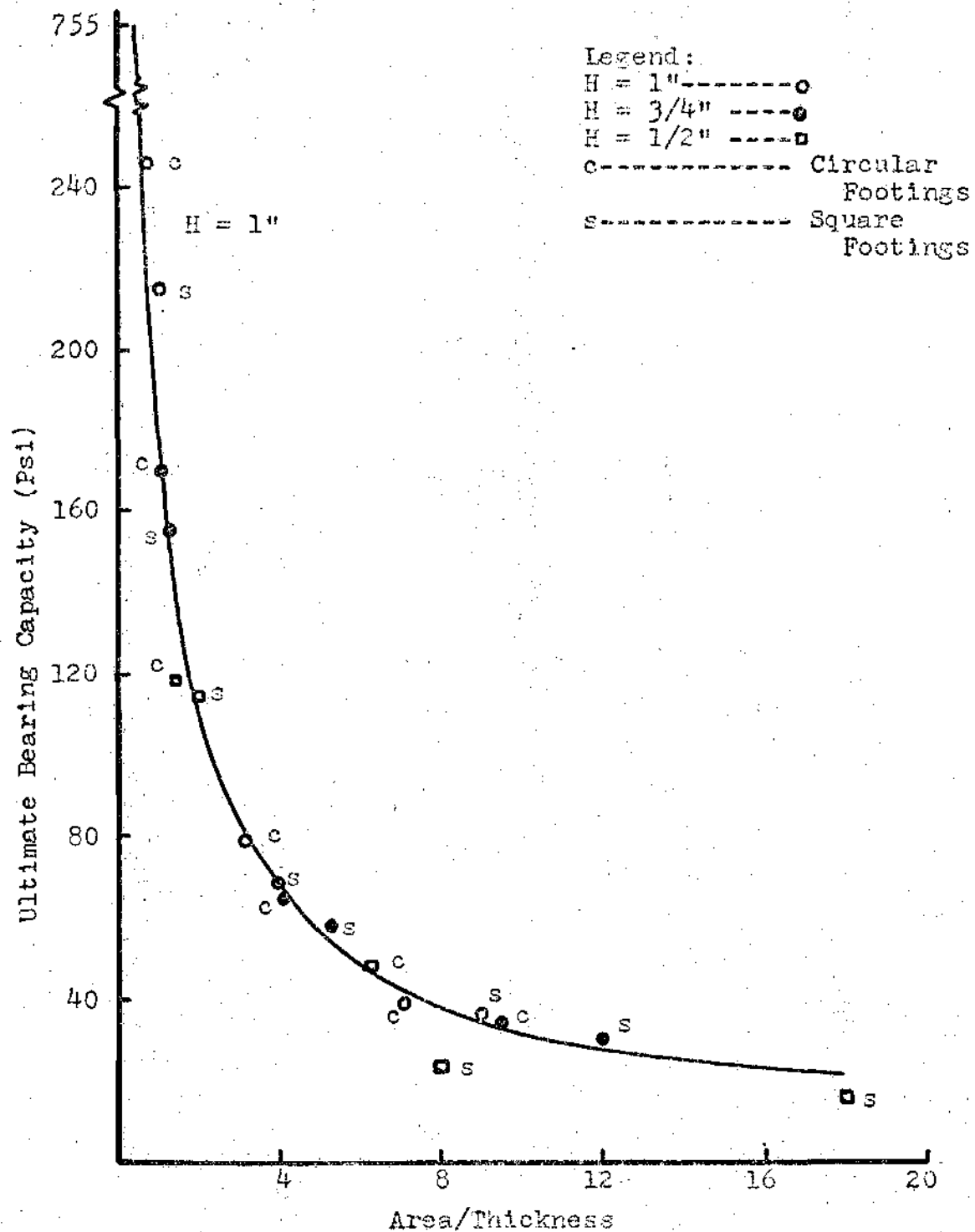


Figure 5: Graph Showing Influence of Footing Area on the Ultimate Bearing Capacity

Mechanism of Failure

Depending on the size of the footing and on the thickness of the hard layer two types of failure occurred.

With the smaller footings, 1 inch in diameter and width respectively and with the thinner slab, 1/2 inch, a punching failure occurred. The footing sank making a hole at the top of the hard layer of the size and shape of the footing (Figures 7, 8) without otherwise fracturing the hard layer. Here, because of the small area of the footing, there is a high stress concentration along the perimeter of the footing which causes this punching failure. Even though the hard layer does not develop much flexural resistance it helps to spread the load over the surface of the clay, since the hole beneath the slab was larger than the footing size, and the surface of failure was like a conical circumferential section inclined at 45° to the vertical. The punching was followed by shear and heave of the clay.

With increasing size of footing the hard layer begins to fail in flexure. As the load on the slab increases, the

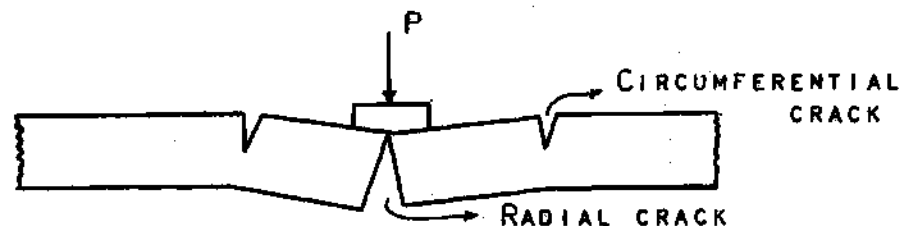
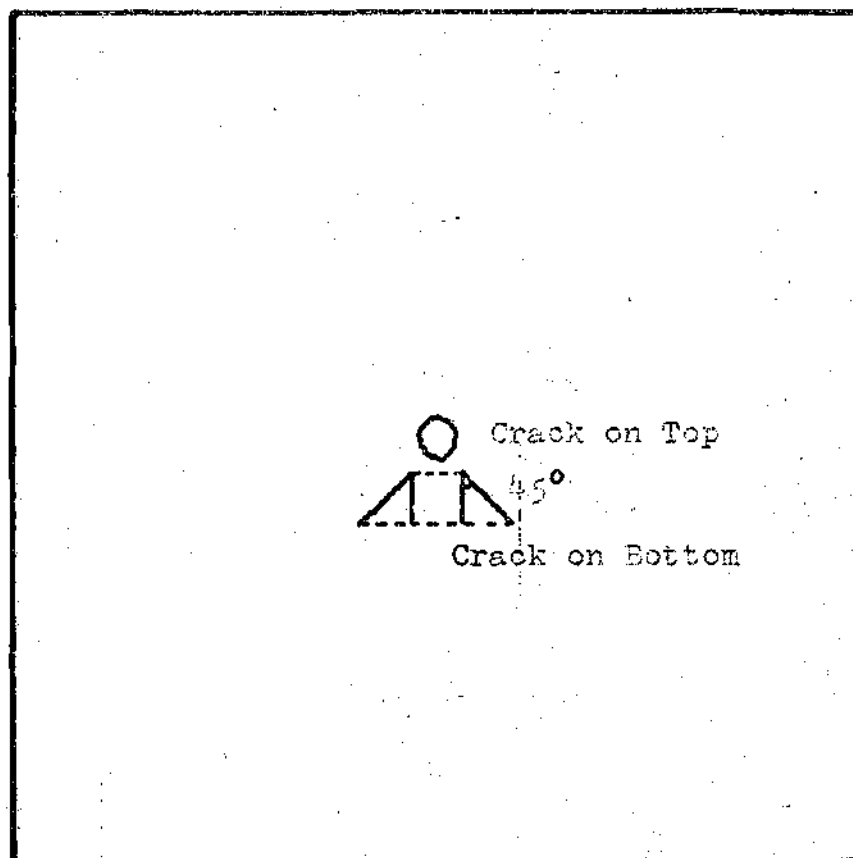
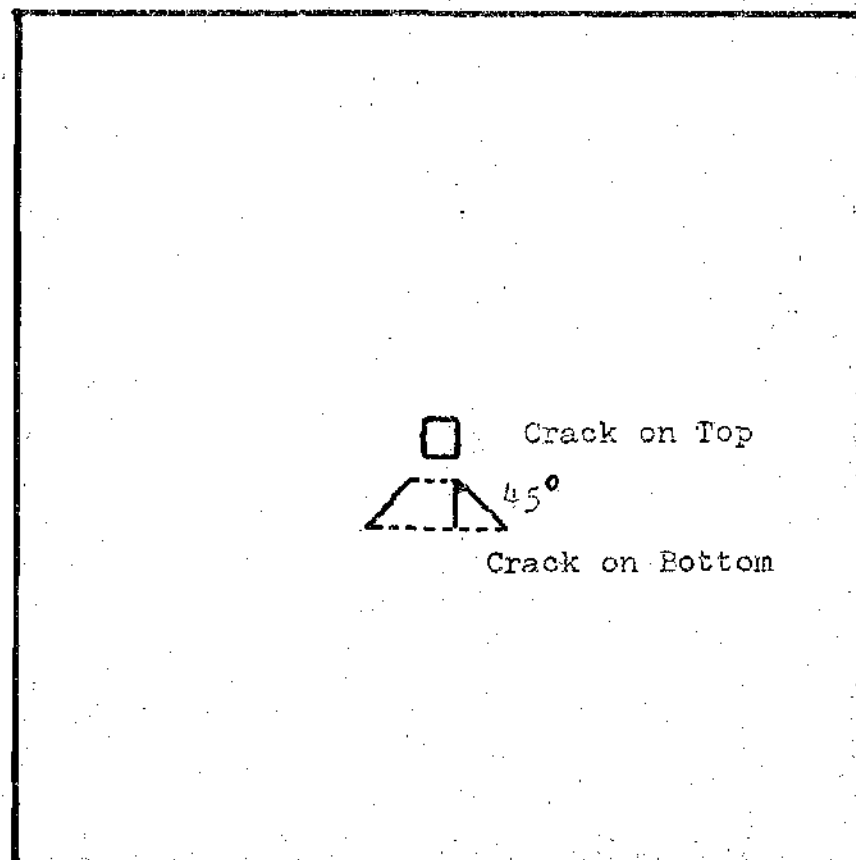


Figure 6: Flexural Failure



Hard Layer Thickness: One-half Inch
Diameter: One Inch

Figure 7: Hard Layer after Failure - Punching Failure

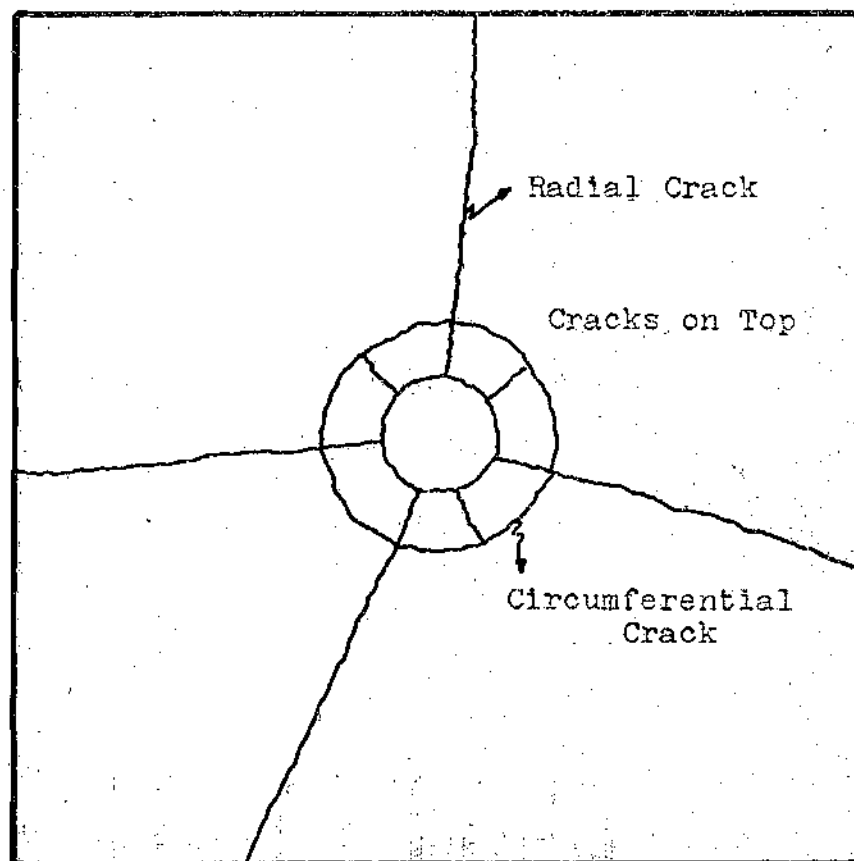


Hard Layer Thickness: One-half Inch
Width: One Inch

Figure 8: Hard Layer after Failure - Punching Failure

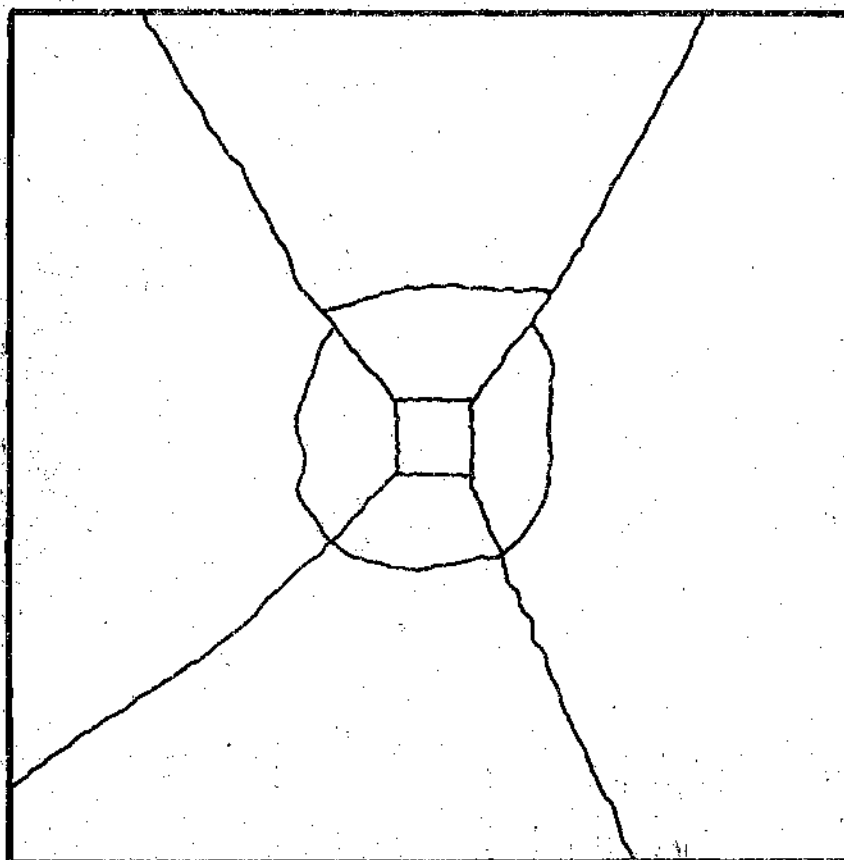
bending stress below the load became equal to the flexural strength of the plaster-sand slab and it begins to yield, leading to radial tension cracks at the bottom. As the load is further increased these cracks appear on the surface of the slab and a circumferential tension crack is formed on top of the slab, Figure 9. After this circumferential crack is formed, complete failure by punching through the slab into the clay occurred, with no increase in load. Figure 9 is a typical example of this type of failure. Some of the slabs did not show a complete circumferential crack, but only a part of one, which may be due to the non-homogeneity of the materials used to make up the two-layer system. Also some of the thicker slabs used, 1 inch, contained after failure only radial cracks which shows that the circumferential moment was not critical. With square footings the radial cracks started always from the corners of the footings, which indicates that there is a high concentration of stresses at these points of the square footings. The circumferential crack was also contained on the slab after failure when square footings were used, as shown in Figure 10.

The concentration of stresses at the corner of the rigid footing is due to the cohesion of the hard layer. This is so, since, if cohesion were zero, the uniform settlement of the rigid footing would produce no pressure at the corners due to the lack of resistance to shear at this point.



Hard Layer Thickness: One-half Inch
Diameter: Three Inches

Figure 9: Hard Layer after Failure - Flexural Failure



Hard Layer Thickness: One-half Inch
Width: Two Inches

Figure 10: Hard Layer after Failure - Flexural Failure

Thickness of Hard Layer

As shown in Figure 4, as the thickness of the hard layer increases the bearing capacity of the system also increases. Regardless of whether the failure is either a punching failure or a flexural failure the ultimate load is increased by increasing the thickness of the hard layer.

Punching Failure

After a failure of this type had occurred, a conical circumferential section inclined approximately 45° to the vertical was contained underside the slab.

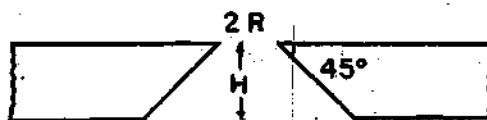


Figure 11. Punching Failure

The lateral area is equal to:

2π (average radius) \times (slant height)

$$\text{Area} = 2\pi \frac{R + (R + H)}{2} \frac{H}{\cos 45^\circ} = (2R + H)\pi \frac{H}{0.707} \quad (9)$$

If the punching resistance is estimated from the vertical component of the total tensile strength (Meyerhof, Ref. 8), f_o , of the slab on the conical circumferential section, we can write

$$P_u = (2R + H)\pi \frac{H}{\cos 45^\circ} f_o \quad (10)$$

Here we see that as the thickness, H , of the hard layer increases, the ultimate punching load also increases.

Flexural Failure

Using Meyerhof's analysis we have from formulas (5) and (7), that is

$$P_o \text{ (collapse)} = \frac{4 M_o \pi}{1 - \frac{R}{3L}} \quad (11)$$

Since

$$M_o = \frac{f_b H^2}{6} \quad (12)$$

Then:

$$P_o = \frac{4 \pi (f_b H^2/6)}{1 - \frac{R}{3L}} \quad (13)$$

It can be seen that as H increases P_o also increases.

Theoretical and Test Results Comparison

In Figure 12 a theoretical curve for formula (11) was drawn, having P_o/M_o as abscissas and R/L as ordinates. The results of the tests were also plotted in the graph, it can be seen that for values of R/L greater than 0.9, the theoretical value of P_o/M_o is smaller than the test results, and for values of R/L less than 0.9 the theory gives somewhat larger collapse loads, or greater P_o/M_o values.

It should be noted, however, that this ratio was determined only for the dimensional relationship used in the

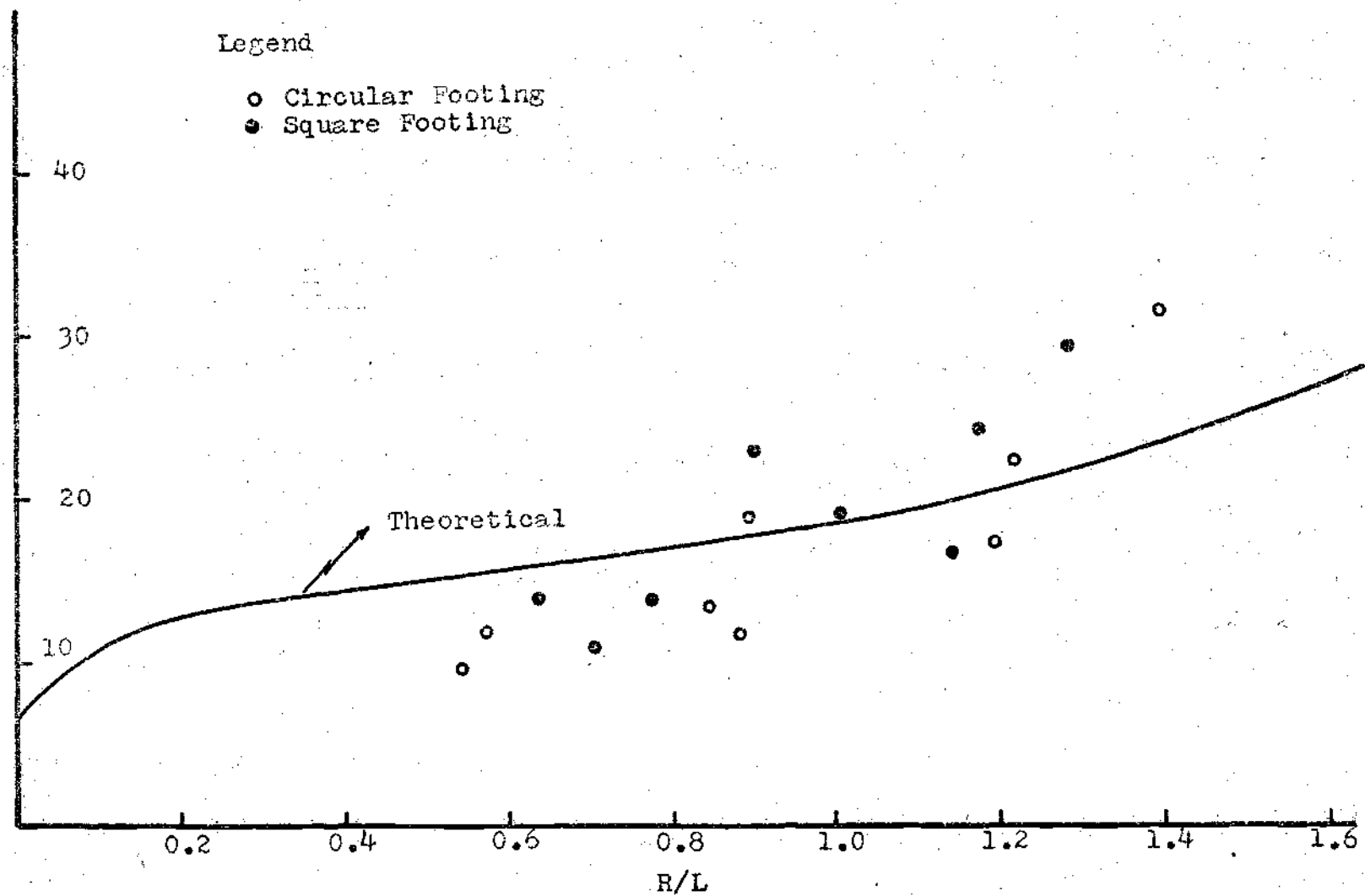


Figure 12: Results of Loading Tests and Theoretical Values

models and may or may not hold true for other conditions. More research is needed to prove or disprove this.

Within the limits of model footings used in this investigation the maximum and minimum values of ultimate bearing capacity that were found were 246 psi and 16.5 psi respectively. The theoretical value for the bearing capacity of the clay alone was 10.5 psi, no experimental value was obtained. The theoretical value for the plaster-sand mixture was 755 psi. Two experimental values for the latter were obtained, using circular and square footings of one inch diameter and width, respectively. For the circular footing an ultimate bearing value of 780 psi was obtained and for the square footing an ultimate value of 745 psi.

Table III gives values for the coefficient of subgrade reaction. These values were determined by the use of a secant line drawn from the origin of the pressure-settlement curves, Appendix II, to a point where the bearing pressure was 50 per cent of the ultimate bearing capacity. With the one inch thick slab, a reduction in the coefficient of subgrade reaction with an increase in area occurred. With the other two slabs the decrease in the coefficient of subgrade reaction with an increase in area is less uniform. From these results there is a slightly indication that the coefficient of subgrade reaction increases as the thickness of the hard layer increases.

Table III: Coefficient of Subgrade Reaction

Thickness of hard layer	Size of footing (inch)	Coefficient of subgrade reaction psi/in
1"	1	8084
	1 x 1	7463
	2	2423
	2 x 2	576
	3	209.5
	3 x 3	582.4
3/4"	1	992.5
	1 x 1	1281.2
	2	2264.5
	2 x 2	707.5
	3	348.5
1/2"	1	1722.4
	1 x 1	1862.5
	2	1491
	2 x 2	257.1
	3	169
	3 x 3	268.3

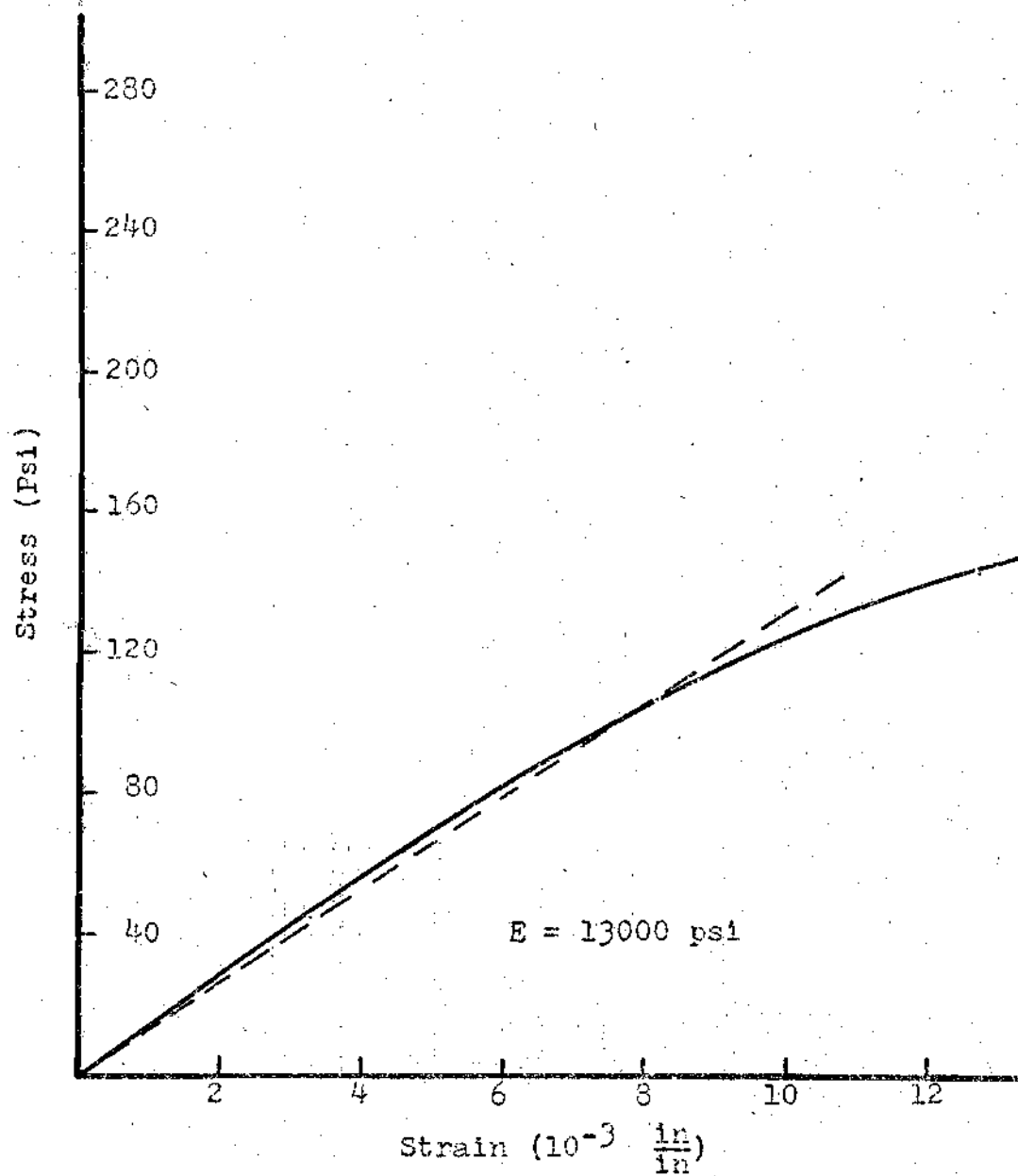


Figure 13: Modulus of Elasticity of the Plaster-Sand Mixture

CHAPTER V

CONCLUSIONS

The conclusions from the results of this work can be summarized as follows:

- (1) The type of failure obtained can, in general, be divided into punching and flexural failure, depending on the thickness of the hard layer and on the size of the footings.
- (2) With square footings the failure or cracking of the hard layer begins always at the corners of the footings.
- (3) The pattern of the curves for ultimate bearing capacity vs. layer thickness, Figure 4, shows that with the bigger footings used the ultimate bearing capacity does not increase, with an increase of the hard layer, as markedly as with the smaller footings. As can be seen the curves tend to flatten out.
- (4) From Figure 5, it can be seen that the ultimate bearing capacity increases in a non-linear manner as the ratio of area of footing to thickness of the hard layer decreases.
- (5) The coefficient of subgrade reaction decreases as the footing area increases. There is also a decrease in the coefficient of subgrade reaction when the thickness

of the hard layer increases. This is believed to happen due to the fact that the rigidity of the system increases as the thickness of the hard layer increases.

CHAPTER VI

RECOMMENDATIONS

1. The load tests that were run in this investigation were with smooth rigid footings. It is recommended that tests be made with flexible footings, to see the influence of stress concentration on the bearing capacity.

2. The influence of the elasticity ratio, or $\frac{E_1}{E_2}$ of the two materials used, over the ultimate bearing capacity should be studied. This can be done by using hard layers of different strength or rigidity keeping the clay at the same water content.

3. Another factor of importance that was not studied here and that can be studied is the effect of shearing-stress build-up that takes place at the interface of the two materials.

4. The effect of the size, cross-section, of the hard layer over the ultimate bearing capacity can be studied by using hard layers of different cross-sections.

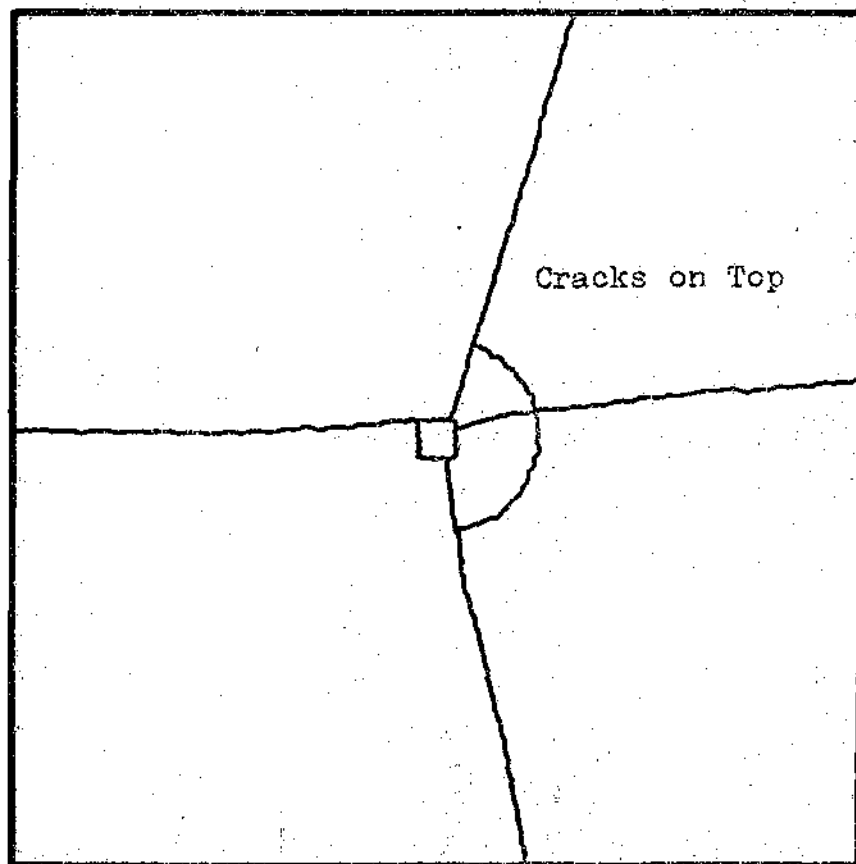
REFERENCES

1. Burmister, D. M., "The Theory of Stresses and Displacements in Layered Systems and Applications to the Design of Airport Runways," Proceedings of the Highway Research Board, Vol. 23, Washington, D. C., 1943, pp 126-148.
2. McLeod, N. W., "Some Basic Problems in Flexible Pavement Design," Proceedings of the Highway Research Board, Vol. 32, Washington, D. C., 1953, pp 90-118.
3. Sowers, G. F., and Vesic, A. B., "Vertical Stresses in Subgrades Beneath Statically Loaded Flexible Pavements," Highway Research Board Bulletin 342, 1962, pp 90-123.
4. Taylor, D. W., Fundamentals of Soil Mechanics, John Wiley and Sons, Inc., 1948.
5. Terzaghi, K. and Peck, R. B., Soil Mechanics in Engineering Practice, John Wiley and Sons, Inc., 1948.
6. Meyerhof, G. G., "The Ultimate Bearing Capacity of Foundations," Geotechnique, Vol. 2, Dec. 1951.
7. Meyerhof, G. G., "Load-Carrying Capacity of Concrete Pavements," Proceedings, ASCE, Vol. 88, No. SM 3, June, 1962, pp. 89-116.
8. Meyerhof, G. G., "Bearing Capacity of Floating Ice Sheets," Proceedings, ASCE, Vol. 86, No. EM 5, October, 1960, pp. 113-145.
9. Westergaard, H. M., "Computations of Stresses in Concrete Roads," Proceedings of the Highway Research Board, Vol. 5, Part I, 1925, pp 90-112.
10. Button, S. J., "The Bearing Capacity of Footings on a Two-Layer Cohesive Subsoil," Proceedings, 3rd International Conference on Soil Mechanics and Foundation Engineering, Vol. I, p 332, 1953.
11. Leonards, G. A. and Haer, M. E., "Analysis of Concrete Slabs on Ground," Proceedings, ASCE, Vol. 85, No. SM 3, June, 1959, pp 35-58.

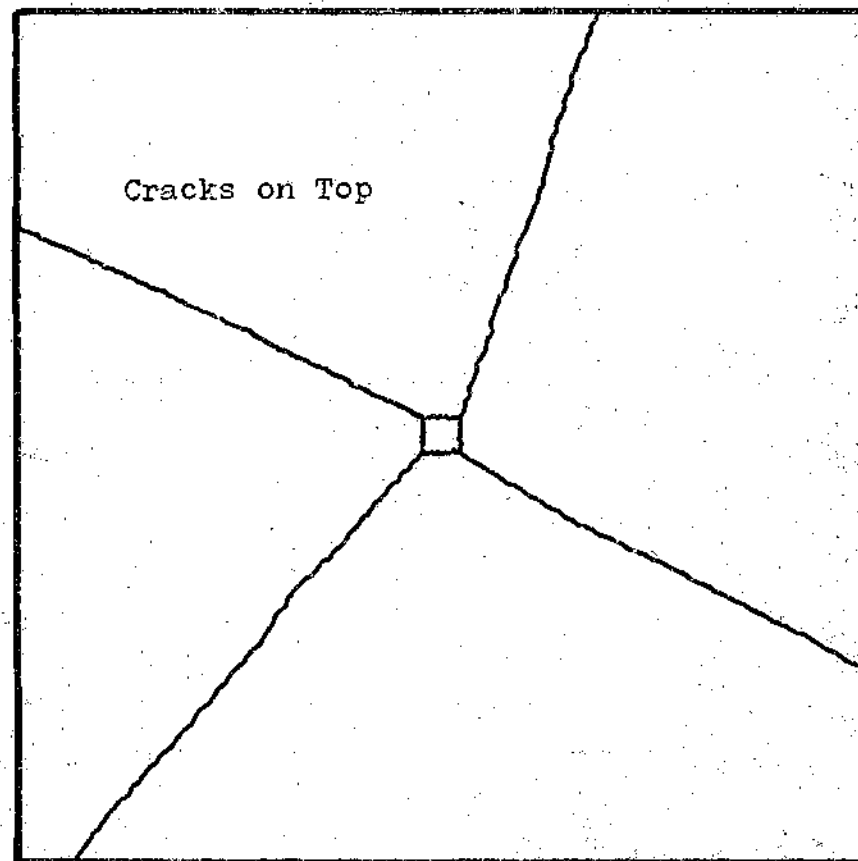
12. Philleo, R. E., "Comparison of Results of Three Methods for Determining Young's Modulus of Elasticity of Concrete," Journal, American Concrete Institute, 51, pp 461-69, Jan., 1955.
13. Gonnerman, H., and Shuman, E. C., "Compression, Flexure, and Tension Tests of Plain Concrete," Proceedings, ASTM, 28, Part II, pp 527-73.

APPENDIX I

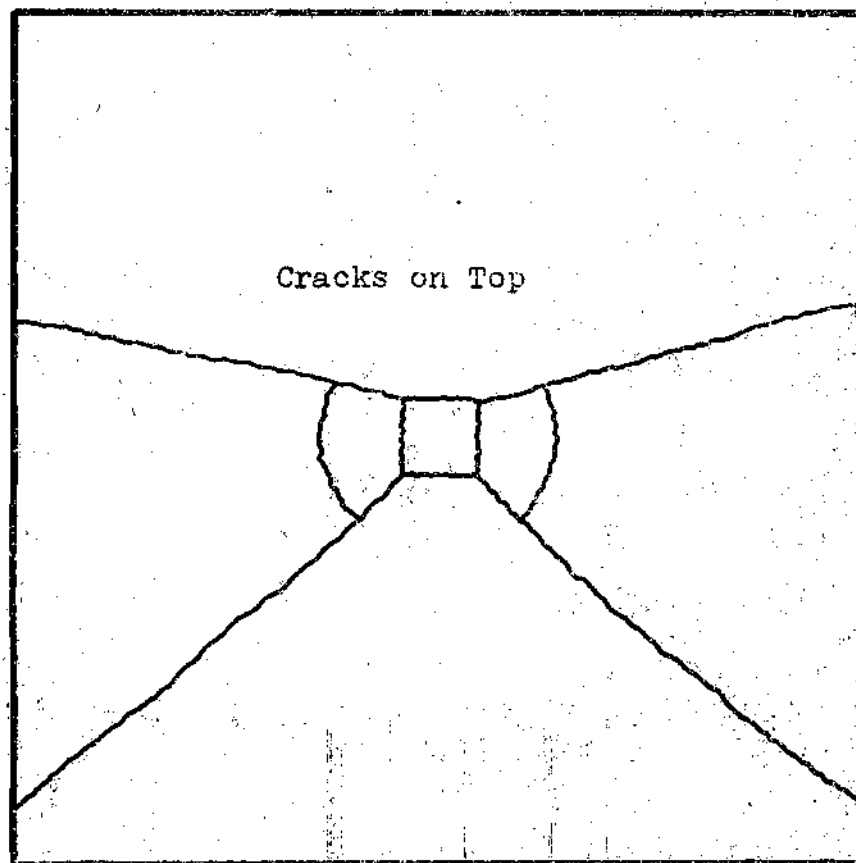
CRACKS ON TOP OF HARD LAYER AFTER FAILURE ACCORDING
TO SIZE OF FOOTING AND THICKNESS
OF HARD LAYER



Hard Layer Thickness: Three-fourth Inch
Width: One Inch



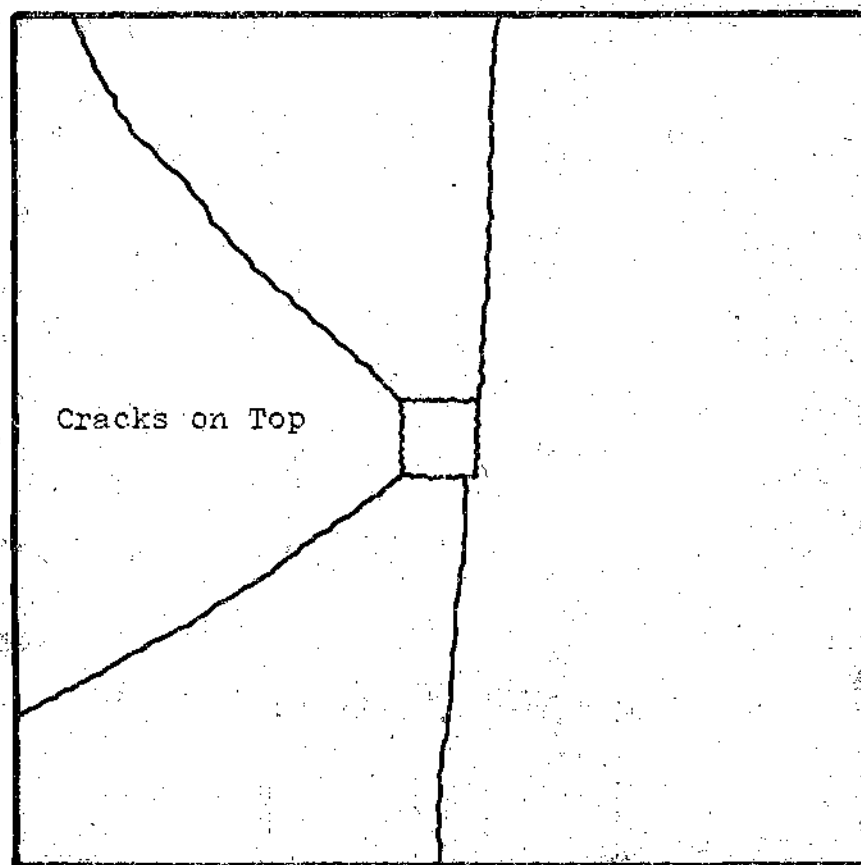
Hard Layer Thickness: One Inch
Width: One Inch



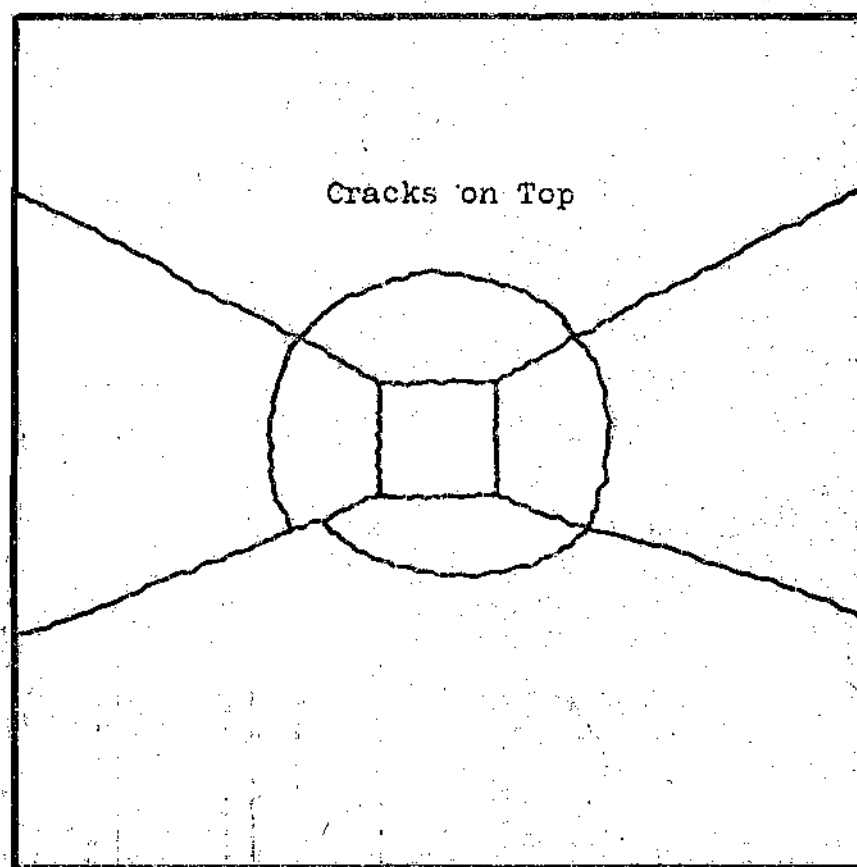
Cracks on Top

Hard Layer Thickness: Three-fourth
Inch

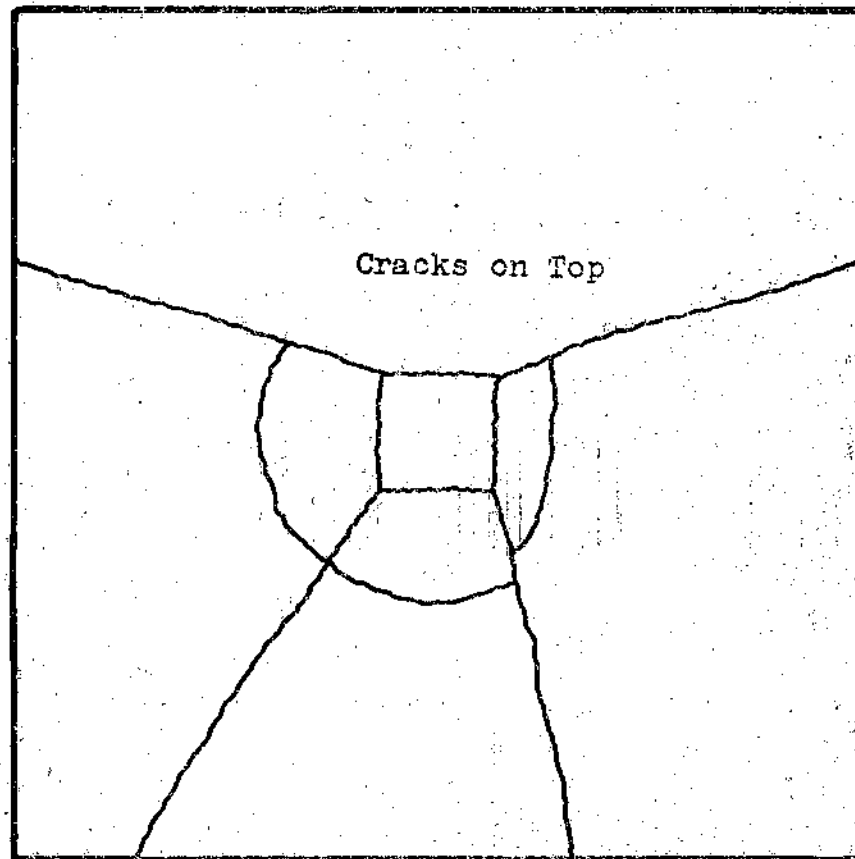
Width: Two Inches



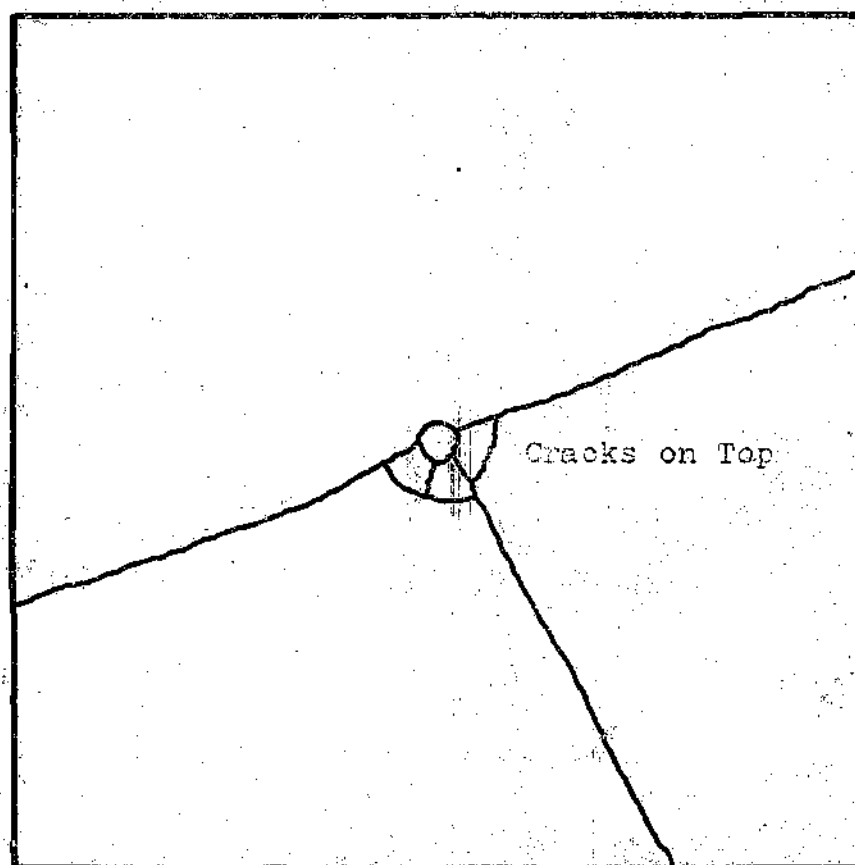
Hard Layer Thickness: One Inch
Width: Two Inches



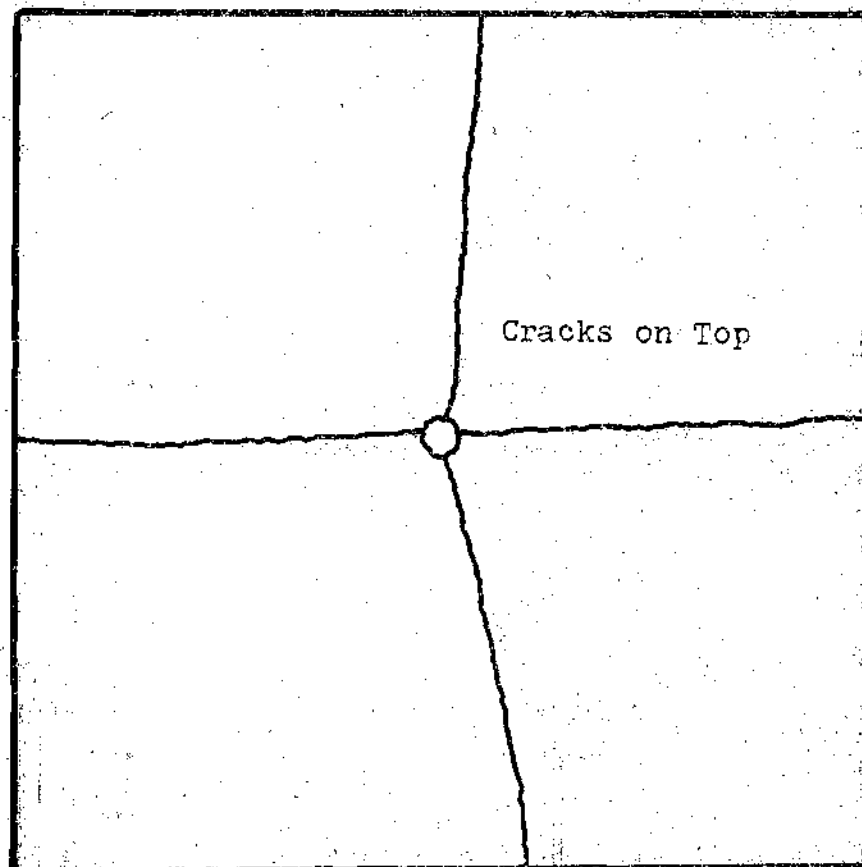
Hard Layer Thickness: One-half inch
Width: Three Inches



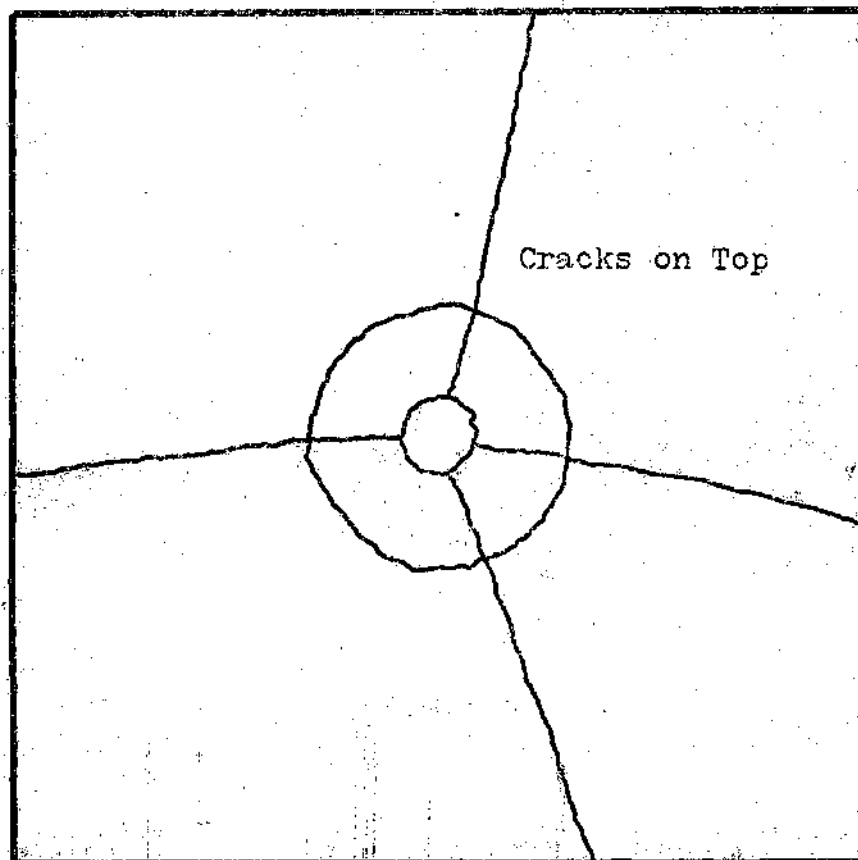
Hard Layer Thickness: Three-fourth Inch
Width: Three Inches



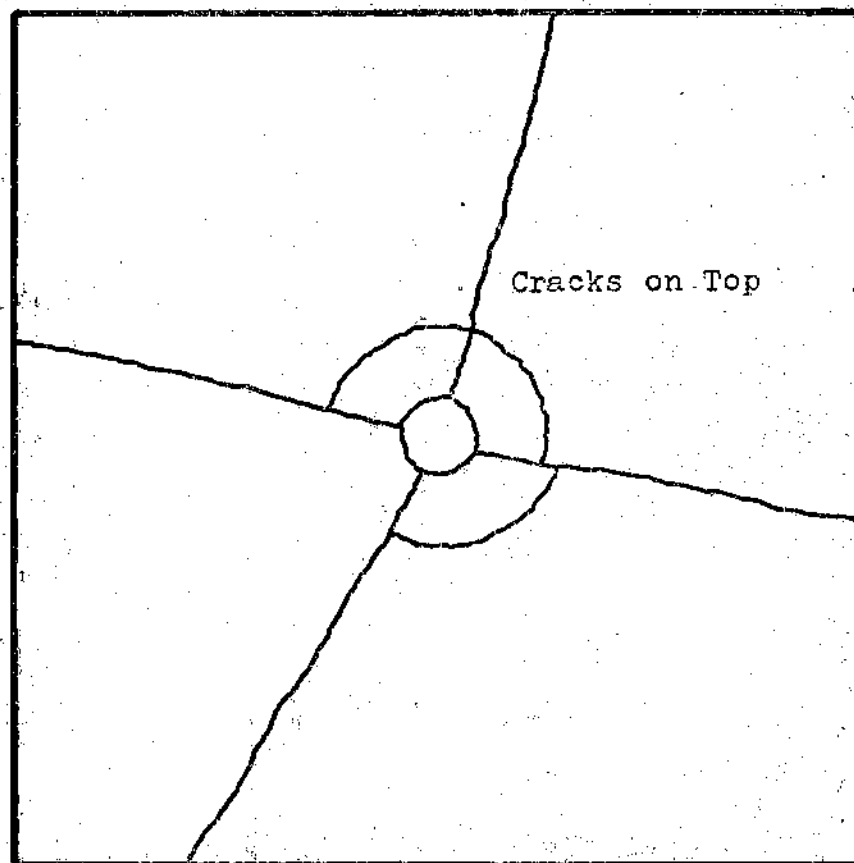
Hard Layer Thickness: Three-fourth Inch
Diameter: One Inch



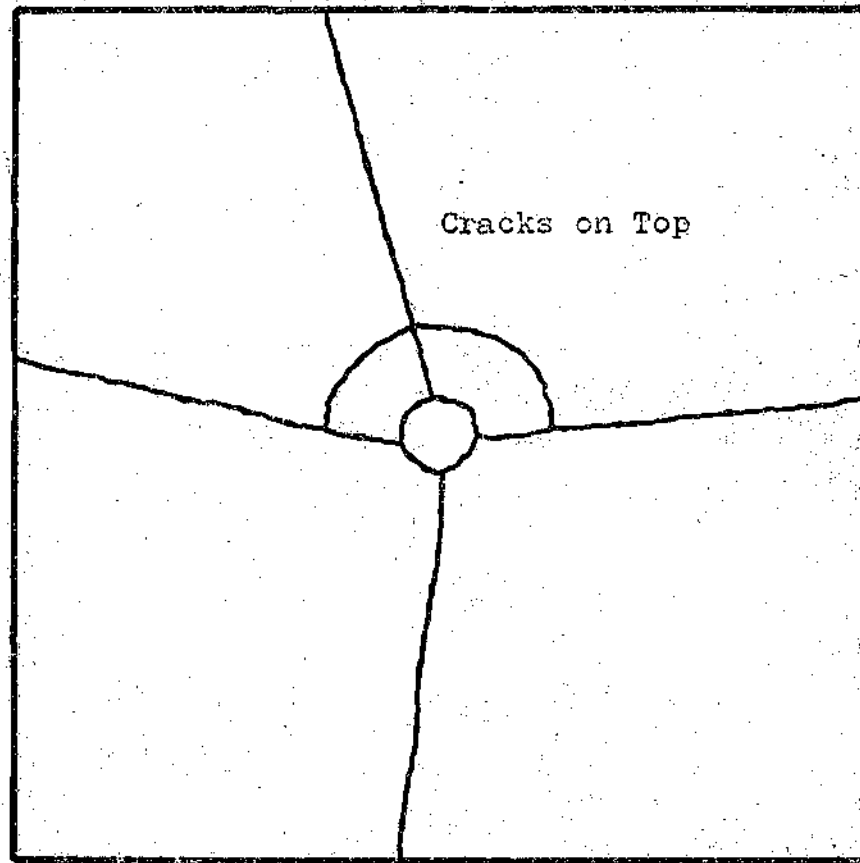
Hard Layer Thickness: One Inch
Diameter: One Inch



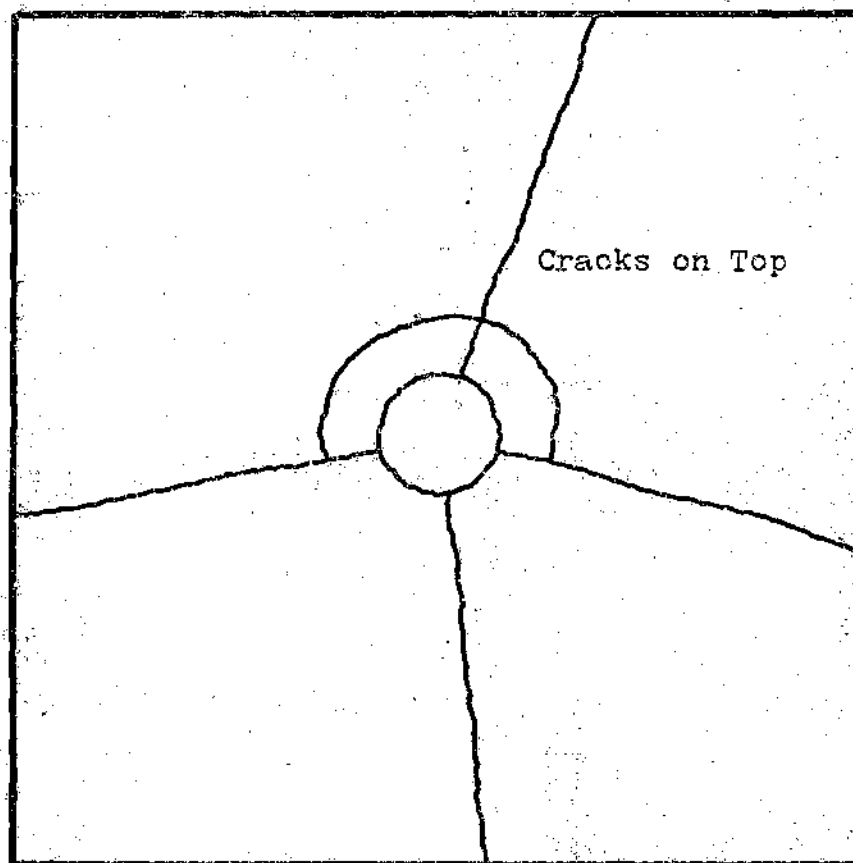
Hard Layer Thickness: One-half Inch
Diameter: Two Inches



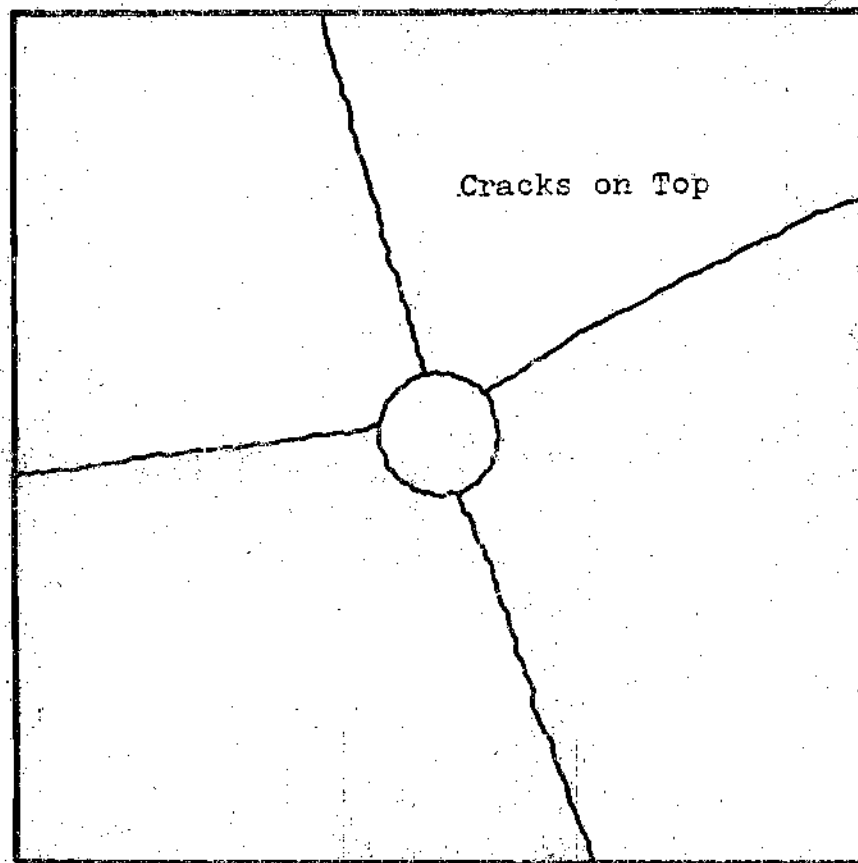
Hard Layer Thickness: Three-fourth Inch
Diameter: Two Inches



Hard Layer Thickness: One Inch
Diameter: Two Inches



Hard Layer Thickness: Three-quarter Inch
Diameter: Three Inches



Hard Layer Thickness: One Inch
Diameter: Three Inches

APPENDIX II

BEARING PRESSURE SETTLEMENT-CURVES

